Estuarine, Coastal and Shelf Science 226 (2019) 106277

Contents lists available at ScienceDirect

Estuarine, Coastal and Shelf Science

journal homepage: www.elsevier.com/locate/ecss

Retrieval of nearshore bathymetry from Sentinel-2A and 2B satellites in South Florida coastal waters

Isabel Caballero*, Richard P. Stumpf

National Centers for Coastal Ocean Science, National Ocean Service, NOAA, Silver Spring, MD, USA

ARTICLE INFO

Keywords:
Satellite-derived bathymetry
Lidar
Copernicus programme
Atmospheric correction
Surface correction

ABSTRACT

This study examines the relatively high-resolution MultiSpectral Instrument (MSI) onboard Sentinel-2A and 2B for generating bathymetric maps through a ratio transform model in South Florida (United States). Atmospheric correction of imagery is implemented though ACOLITE software, providing accurate performance and consistency over different Sentinel-2A/B scenes and three different study sites. Vertical calibration uses 5–10 points collected from digital charts, independent of lidar surveys, which are used for validation and error analysis. Satellite-Derived Bathymetry (SDB) has Median Absolute Error (MedAE) of 0.5 m in West Palm Beach (at depths ranging between 0 and 18 m, limit of lidar survey for validation), 0.4 m in Key West (0–5 m), and 0.22 m in Dry Tortugas (0–6 m), in conditions with low turbidity. Accurate bathymetry mapping can be accomplished with both sensors over environments with varying water transparency conditions, with the advantage of a fast, flexible, and economical solution. The 10-m MSI can capture small-scale features, such as tidal channels, straits relevant to navigation or steep slopes. While the least error is achieved by calibrating each image separately, a generic calibration produces only a moderately greater error with MedAE still ~1m, indicating the robustness of the approach. The research highlights the great potential of the 5-day revisit, suggesting that the twin Sentinel-2 mission of the Copernicus programme may enhance SDB to leverage its use for several operational purposes, particularly in remote and inaccessible regions of the world.

1. Introduction

Accurate and high-resolution information on bathymetry is critical for a wide range of coastal purposes such as navigation, dredging planning, environmental management, aquaculture, and mapping benthic habitats. In addition, bathymetric surveys are increasingly important for understanding the effects of climate change on the environment, alerting scientists to areas with potential for erosion, as well as impacts of sea-level rise and subsidence (Culver et al., 2010). Traditional means of determining water depth include the conventional vessel-based multi-beam sonar or active non-imaging airborne lidar bathymetry (ALB). Sonar surveys generate precise depths at sampling points that meet hydrographic surveys standards. (Guenther, 2011); however, they are constrained by access, speed, deployment cost and efficiency in shallow waters. ALB allows for the acquisition of safe, rapid and reasonably accurate high-resolution bathymetric information in moderately clear nearshore waters, especially in shallow water where multi-beam is least effective. While Satellite-Derived Bathymetry (hereinafter SDB) does not have the accuracy of sonar or lidar, it can provide wide swaths, low-cost repeated coverage, and easy access to remote locations for reconnaissance mapping (Robinson et al., 2000; Gao, 2009). SDB has recently emerged as another powerful tool to help the National Oceanic and Atmospheric Administration (NOAA) address the public expectation for rapid updates to nautical charts in order to insure safe navigation in United States waters (Pe'eri et al., 2012).

Since the first studies in the late 1970s, a number of researchers have attempted to determine comprehensive regional SDB with several passive systems (typically Landsat but extended to any sensor) to varying degrees of success (Lyzenga, 1981; Benny and Dawson, 1983; Philpot, 1989; Maritorena et al., 1994). Over these last decades, the suitability of remotely sensed satellite data for mapping bottom depth has been confirmed and refined with the successive advancements in optical platform resolution and SDB models (Gao, 2009; Dekker et al., 2011; Bramante et al., 2013). Studies have reported a reduction in error from approximately 30% from multispectral data (Philpot, 1989) to less than 15% from hyperspectral aerial data (Brando et al., 2009). When using multispectral imagery, optically based approaches have been regularly used to estimate bottom depth from the optical properties of water and underwater reflectance (Lyzenga, 1981; Philpot, 1989; Stumpf et al., 2003; Minghelli-Roman et al., 2009). Various studies

* Corresponding author.
E-mail address: Isabel.caballero@icman.csic.es (I. Caballero).

https://doi.org/10.1016/j.ecss.2019.106277
Received 29 November 2018; Received in revised form 21 June 2019; Accepted 27 June 2019
Available online 28 June 2019
0272-7714/ © 2019 The Authors. Published by Elsevier Ltd. This is an open access article under the CC BY-NC-ND license (http://creativecommons.org/licenses/BY-NC-ND/4.0/).

have used analytical approximations of the radiative transfer model for light propagation in water to determine depth (Benny and Dawson, 1983; Clark et al., 1988; Lyzenga et al., 2006: Dekker et al., 2011). Optimization of semi-analytical algorithms has been developed with hyperspectral imagery, allowing determination of many water constituent concentrations and depth simultaneously (Lee et al., 1999, 2007). These optimization solutions have also been applied to multispectral data to solve simultaneously for depth, benthic albedo, cover and water optical properties (Hamylton et al., 2015; Hedley et al., 2018), but they require the parameterization of reflectance spectra of main benthic habitats, basic information about water properties, and extremely accurate atmospheric correction. Current atmospheric correction methods do not consistently produce sufficiently accurate water reflectance, which makes them inefficient from an operational or recursive monitoring point of view (Dekker et al., 2011; Hedley et al., 2018). These methods are also more complex to implement and can be computationally slower.

Several SDB experiments have been chiefly applied to oligotrophic waters or have been modified to incorporate additional in-situ data (Lafon et al., 2002; Gao, 2009; Kao et al., 2009; Minghelli-Roman et al., 2009). Many of these methods depend on either extensive field data information (limited or nonexistent in most cases) or research sensors (like hyperspectral), which are not practical for routine application. In 2003, Stumpf et al. published a model for determining bathymetry over shallow reefs and atolls applying a ratio transform instead of a linear transform. The method was designed to support routine mapping in areas with extremely limited calibration data. Recent studies exhibited the great potential of this model for bathymetry mapping in several regions worldwide (e.g. Halls and Costin, 2016; Islam et al., 2016; Chybicki, 2017). Kabiri (2017b) demonstrated that the ratio transform method has more proficiency in determining depth values in coastal water bodies with a high variation in bottom types, whereas using the linear transform methods may lead to less accurate results. In addition, Hamylton et al. (2015) developed a comparison of the band ratio and optimization approaches for estimating SDB in Australia revealing that these methods yield very similar estimates overall, and both were subject to the same depth limitations mainly associated with the site water characteristics.

The application of high spatial resolution imagery such as IKONOS, QuickBird and the family of WorldView satellites can offer accuracy and a detailed monitoring (Stumpf et al., 2003; Eugenio et al., 2015; Hamylton et al., 2015; Halls and Costin, 2016). Nevertheless, these observations are quite limited in areal coverage, frequency, and cost. On the contrary, the free of charge Landsat (30 m) imagery can be utilized to yield reliable and updated SDB, especially since the launch of Landsat-8 in 2013 (Pe'eri et al., 2014; Pacheco et al., 2015; Kabiri, 2017a). More recently, the European Space Agency (ESA) launched the Sentinel-2 twin mission as part of the Copernicus programme. The two operational satellites (A/B) offer a potential 5-day revisit time with their Multi Spectral Imagers (MSI) at 10, 20 and 60 m spatial resolution. While this mission was intended for global monitoring of land, it has already led to investigation of nearshore and inland water parameters (Toming et al., 2016; Vanhellemont and Ruddick, 2016; Martins et al., 2017; Caballero et al., 2018). Compared to Landsat-8, Sentinel-2 has three additional spectral bands within the near infrared (NIR) region (red-edge bands), enabling further insights into water quality examination over optically complex coastal/inland waters such as chlorophyll-a or turbidity (IOCCG, 2000; Ruddick et al., 2016; Vanhellemont and Ruddick, 2016; Pahlevan et al., 2017b). A study by Pahlevan et al., (2017a, b) confirmed MSI radiometric performances are comparable to those of the Lansdat-8 Operational Land Imager (OLI), highlighting the high-quality products that can be derived from Sentinel-2. Furthermore, recent works already demonstrated the feasibility of Sentinel-2A to map bottom depth with several degrees of success (Chybicki, 2017; Kabiri, 2017b; Traganos and Reinartz, 2017; Hedley et al., 2018 ; Casal et al., 2019). As such, the potential to generate continuous bathymetry from

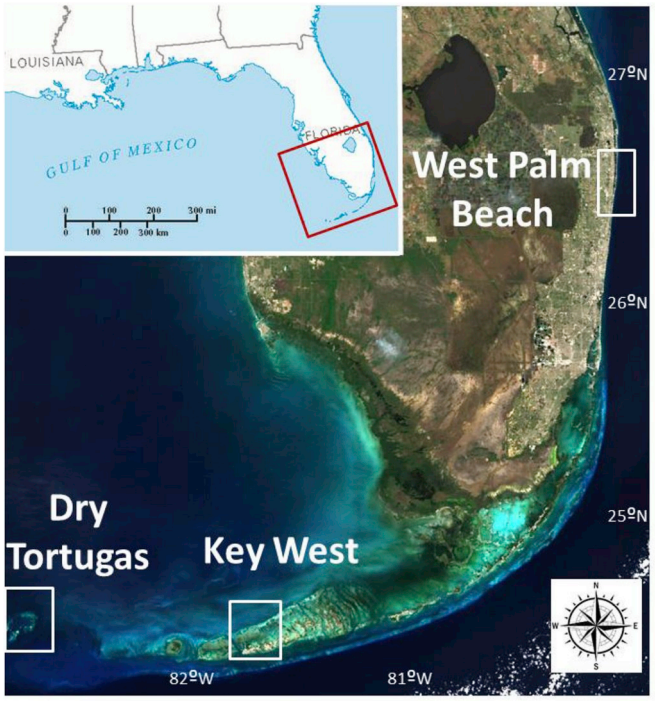

Fig. 1. Location of the study regions in South Florida coastal waters (United States).

Sentinel-2 has become a topic of increased interest for coastal monitoring in the framework of the Copernicus programme. Therefore, the goal of this study was to investigate the performance of the SDB method with both Sentinel-2A and 2B for retrieving bathymetry in nearshore waters with some turbidity. The paper focused on the application of an atmospheric correction scheme and the vertical calibration procedure to assess the quality of performance and repeatability over different scenes and three study sites in United States.

2. Materials and methods

2.1. Study region

The areas under investigation included three specific study sites in South Florida (SF): Dry Tortugas, Key West, and West Palm Beach (Fig. 1). For method development and testing, these regions were selected as we had available updated lidar data for comparison and error analysis. In addition, the locations were chosen based on the general conditions of low to medium turbidity, with lowest turbidity levels occurring in the Tortugas segment (Jones and Boyer, 1998).

The Dry Tortugas (24° 38' 0" N and 82° 55' 1" W, Fig. 1) is a small archipelago of coral islands located in the Gulf of Mexico at the end of the Florida Keys. The islands, with their surrounding waters, reefs and submarine banks, constitute the Dry Tortugas National Park, which is part of the Everglades & Dry Tortugas Biosphere Reserve, established by UNESCO in 1976 under its Man and the Biosphere Programme. Existing habitats have been classified based on habitat relief and patchiness describing nine hard-bottom, soft-sediment and coral reef habitats encountered from 1 to 33 m depth (Franklin et al., 2003).

Key West is an island in the Straits of Florida, at the southernmost tip of the Florida Keys (24° 33′ 25″ N and 81° 47′32″ W, Fig. 1). The Florida Keys are a limestone archipelago with a total land area of 356 km^2 and are one of the most touristic regions in the United States. Much of the population is concentrated in a few areas of higher density, such as the city of Key West, which has 32% of the entire population of the Keys. Strong gradients in water quality have been identified according to distance from shore, with offshore waters being the clearest

and most oligotrophic (LaPointe and Clark, 1992; Barnes and Hu, 2013). The generally shallow water depth (0–6 m) presents the potential for frequent resuspension of suspended solids. The basins also have varying substrates and (carbonate) sediment types (Fourqurean et al., 1992), which affect the nature and concentration of suspended solids in the water column. The diverse substrates vary from sand to pavement, with cover that includes various densities of seagrass (from dense to bare bottoms) and some coral patches.

West Palm Beach is a National Historic Landmark located on the Palm Beach barrier island, in SE Florida (26° 42′ 14″ N and 80° 02′08″ W, Fig. 1). The eastern Florida Shelf is extremely narrow (3–4 km) and merges southward with the Florida Reef Tract, which is most extensive and best developed offshore from the Florida Keys. The study area corresponded to a coastal strip in central eastern Palm Beach County. Portions of the Florida east coast differ markedly in shoreline configuration and are influenced by the tectonic setting of the continental margin, regional bedrock geology, nearshore sediment supply, and relative sea-level fluctuations during the Quaternary (Duane and Meisburger, 1969; Benedet et al., 2004). The geomorphology of this area consisted of a wide range of bottom types that included coral reefs, hard rounds (rock reefs), and sedimentary features including bar and trough systems as well as sandy bottom types (Finkl and Warner, 2005).

2.2. Satellite data: Sentinel-2A/B mission from the Copernicus programme

ESA has developed the Sentinel fleet to meet the operational needs of the Copernicus programme, the European Commission's Earth Observation Programme. Each Sentinel mission is based on a constellation of two satellites to fulfill revisit and coverage requirements, providing robust data sets for Copernicus services. In this study, Sentinel-2A and 2B twin polar-orbiting satellites were used (European Space Agency, 2015). Sentinel-2A was launched on 23 June 2015 and Sentinel-2B followed on 7 March 2017 with Sentinel-2A first becoming available in this area in October 2015, and routine collection of data at 10-day repeat a year later. The radiometric resolution of MSI is 12-bit, and spectral and spatial characteristics of the bands used in this study are shown in Table 1. Sentinel-2 scenes for SF region were downloaded from the Sentinel's Scientific Data Hub. These images corresponded to Level-1C (L1C) products processed by the Payload Data Ground Segment (PDGS), which means data were radiometrically and geometrically corrected Top Of Atmosphere (TOA) products. The corrections included orthorectification and spatial registration on a global reference system (combined UTM projection and WGS84 ellipsoid) with sub-pixel accuracy (European Space Agency, 2015). In this study, the images of zone 17 in Dry Tortugas (sub-tile RLH), Key West (sub-tile RMH), and West Palm Beach (sub-tile RNK) were used, with different acquisition plans for each region. Only scenes with low cloud coverage and sun glint were selected for further analysis. The analysis focused on scenes before Hurricane Irma (September 2017) since intense resuspension and currents may have modified shallow seabed morphology, confounding comparison and validation with the lidar surveys (all collected before September 2017). However, additional imagery after Irma was selected for examination of Sentinel-2A and 2B comparability since the first images offered with Sentinel-2B in this region were after the hurricane.

Table 1
Sentinel-2 spectral band settings used in this study indicating central wavelength, width, spatial resolution, and associated Signal to Noise ratio (SNR) at reference radiance (see Drusch et al., 2010).

	Sentinel-2 (MSI)			
	Central wavelength (nm)	Spatial resolution (m)	Bandwidth (nm)	SNR
B01	444	60	20	129
B02	490	10	65	154
B03	560	10	35	168
B04	664	10	30	142
B05	704	20	15	117
B06	740	20	15	89
B07	783	20	20	105
B8A	865	20	20	72

Sentinel-2 images were processed to Level-2A (L2A) by using the robust ACOLITE processor developed by the Royal Belgian Institute of Natural Sciences (RBINS), which supports free processing, specifically for aquatic applications, of both Landsat-8 and Sentinel-2 (Ruddick et al., 2016; Vanhellemont and Ruddick, 2016). Realistic spatial patterns of MSI-derived marine reflectance have been retrieved with ACOLITE allowing proper evaluation of potential applications in coastal and inland waters (Vanhellemont and Ruddick, 2016; Martins et al., 2017). ACOLITE products corresponded to Remote sensing reflectance (Rrs, 1/sr) in all visible and Near-infrared (NIR) bands resampled to 10 m pixel size. Given the conditions of moderate turbidity in the areas under investigation, a combination of the NIR and Short Wave Infrared (SWIR) channels was used for atmospheric correction in ACOLITE. We selected the NIR/SWIR (0.8/1.6 μm) bands for the aerosol correction with a user defined epsilon value (maritime aerosol) recommended in low to moderate turbidity waters. This strategy has been shown to significantly improve the quality of the products by minimizing the influence of NIR/SWIR instrument noise (Pahlevan et al., 2017b). ACOLITE outputs showed some specular noise (speckle noise) and inter-pixel variability so a spatial filter (median filter 3x3) was conducted on the bands in order to remove or diminish this effect.

2.3. In-situ data: airborne lidar bathymetry

The National Geodetic Survey (NGS) collected topographic and bathymetric (topobathy) airborne lidar bathymetry (ALB) in Key West (April 2016), West Palm Beach (February 2017), and Dry Tortugas (October 2016). These point cloud data were collected using the Riegl VQ-880-G sensor, which provided high-resolution bathymetric data in nearshore waters. The Riegl VQ-880-G used a green laser that operated in a circular scan pattern, which could penetrate shallow (clear) water to the seafloor. The high-density point data was combined with GPS and other positional data to create precise 3D topobathy elevation models. NGS used coastal elevation data to map the mean high-water shoreline, which is considered the nation's official shoreline. These high-resolution observations (1 m spatial resolution) were selected as the reference data set in the well-controlled study sites and compared to SDB products. ALB data in Key West corresponded to optically shallow waters ranging from 0 up to 8 m. This region contained several tidal and dredged channels and bottom irregularities that were detectable with ALB, allowing some examination of the MSI capacity to map these irregular bottom types. In West Palm Beach, depths surveyed ranged from 0 up to 18 m, and in the Dry Tortugas region, mapped depths ranged from 0 to 8 m. All ALB data sets were referenced to the Mean Lower Low Water (MLLW) and gridded at the MSI's image resolution (10 m) via arithmetic averaging.

2.4. Satellite-Derived Bathymetry estimation

One common method for deriving bathymetry from satellite imagery is a nonlinear solution using a band ratio calculation (Stumpf et al., 2003). The model uses a ratio of log-transformed water reflectance of bands having different water absorptions, so the ratio of reflectances will change with depth. The log-transform accounts for the exponential decrease of light with depth. Blue light (440–500 nm) can penetrate to at least 25 m depth, and thus provides the optimal reference band for extracting depth information against the more rapidly absorbed green or red light. As red attenuates faster than green it may provide more information in water shallower than 6–8 m. Recent works with the introduction of WorldView-2's higher resolution coastal blue band (400–450 nm) have shown that accurate bathymetric estimations could

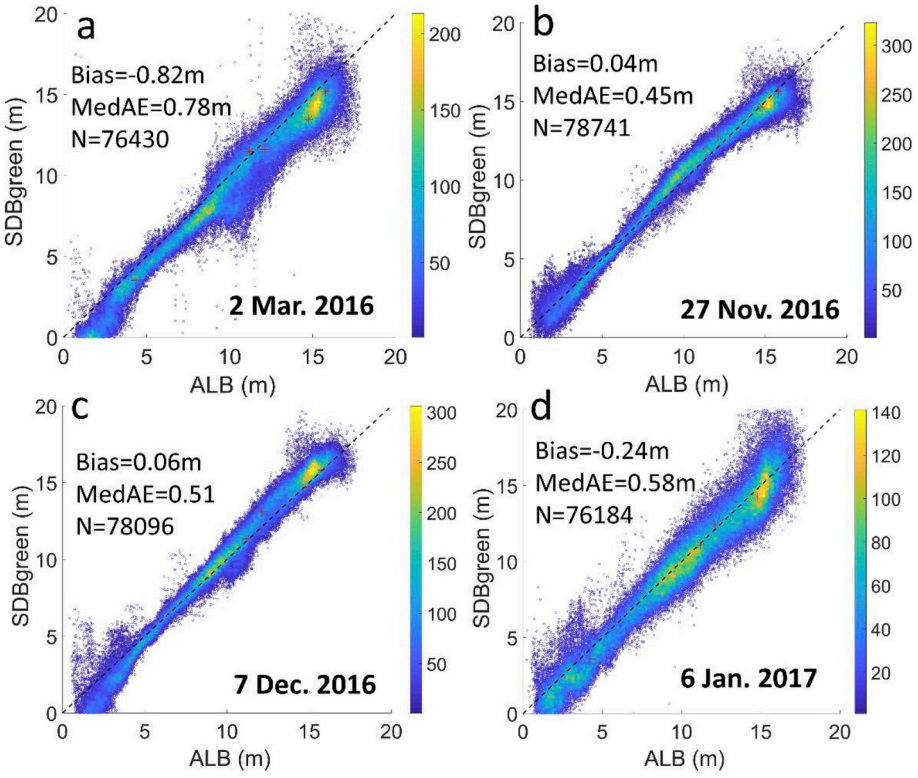

Fig. 2. Scatterplot between ALB and MSI-derived SDBgreen using band 445 nm for the West Palm Beach scenes acquired on (a) 2 March 2016, (b) 27 November 2016, (c) 7 December 2016, and (d) 6 January 2017. Dark dotted lines indicate 1:1 lines.

be achieved up to 20 m and deeper (Bramante et al., 2013; Jawak et al., 2015; Khondoker et al., 2016) as well as with Landsat-8 (Kabiri, 2017a). The coastal blue band is least absorbed by water and designed to improve feature classification and bathymetry measurements (Staff, 2013), at least in waters with low colored dissolved organic matter. However, Kanno et al. (2014) suggested this band was of lower performance although it was intended for use in SDB. Given that Sentinel-2 has two blue bands (Table 1), the model was tested using coastal blue B01 (hereinafter 445 nm) and blue B02 (hereinafter 490 nm) as the numerator (Equation (1)). Therefore, we used the ratio of 445 nm or 490 nm (λ_i) to 560 nm (λ_j) bands, and the ratio of 445 nm or 490 nm (λ_i) to 664 nm (λ_j) bands

$$\mathrm{SDB} = m_1 \mathrm{pSDB} - m_0 \tag{1}$$

$$\text{where pSDB} = \frac{\ln(n\,\pi\,\mathrm{Rrs}(\lambda_i))}{\ln(n\,\pi\,\mathrm{Rrs}(\lambda_j))}$$

where pSDB is the relative or "pseudo" depth from satellite (dimensionless), SDB is the satellite-derived depth (meters), referred to as either SDBgreen for λ_j = 560 nm, or SDBred for λ_j = 664 nm, m_1 and m_0 (scale and offset, respectively) are tunable constants to linearly transform the algorithm results to the actual depth in a chart, and n = 1000 is a fixed constant for all areas to assure that both logarithms will be positive under any condition and that the ratio will produce a linear response over the retrievable water depth.

2.5. Vertical tuning

After calculating pSDB, the first step was to tune the algorithms by means of the vertical referencing to linearly transform the results to the actual depth defining the scale and offset (m_1 and m_0, respectively; Equation (1)). As this model has only two coefficients that require tuning, few calibration points are needed (Stumpf et al., 2003). To further test the robustness of the method, depths were obtained from the chart soundings, not from the lidar used for validation. Control points were extracted from NOAA charts. Charts corresponded to 11441-11442 for Key West (the depth range of the calibration points was 0–5 m), 11472-11467 for West Palm Beach (the depth range of the calibration points was 0–21 m), and 11434-11438 for Dry Tortugas (the depth range of the calibration points was 0–8 m). This procedure is significant for evaluating a precise approach that can be replicated in remote areas or regions without requirement of high-resolution bathymetry. Five to ten control points were identified from the charts, defining stable points in low gradient areas, and avoiding areas that could have been modified. Each scene and algorithm were tuned separately, with correlation calculated as a quality indicator. A single calibration for all scenes was examined also in West Palm Beach. The coefficients were retrieved testing both 445 nm and 490 nm bands. The pSDB was then scaled to SDB with linear regression between the reference chart bathymetry and pSDB. South Florida coastal waters corresponded to a micro-tidal system (https://tidesandcurrents.noaa.gov/). The m_0 coefficient provides an adjustment to the reference bathymetric datum in charts (MLLW), implicitly correcting for tide (water level).

3. Results

3.1. Validation of Satellite-Derived Bathymetry products

In order to verify MSI capacity to generate bottom maps at 10 m and evaluate its performance in relation to high-resolution lidar data, an analysis of the two models SDBred and SDBgreen compared to ALB observations was performed. In this section, only Sentinel-2A satellite (before Hurricane Irma, September 2017) was used for validation purposes and the results were organized for each study site and SDB model: both SDBred and SDBgreen in West Palm Beach and SDBred over the shallow regions of Dry Tortugas and Key West.

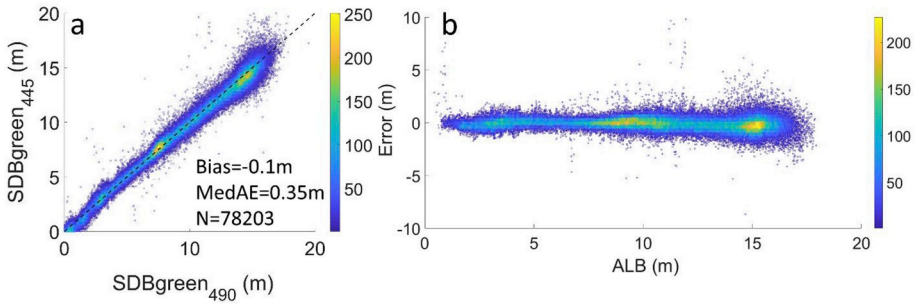

Fig. 3. (a) Scatterplot between MSI-derived SDBgreen using band 490 nm against SDBgreen using band 445 nm for the Wet Palm Beach scene acquired on 2 March 2016, where dark dotted line indicates 1:1 line, and (b) Comparison of ALB against total error between SDBgreen using both blue bands ($SDBgreen_{445}$-$SDBgreen_{490}$). (For interpretation of the references to color in this figure legend, the reader is referred to the Web version of this article.)

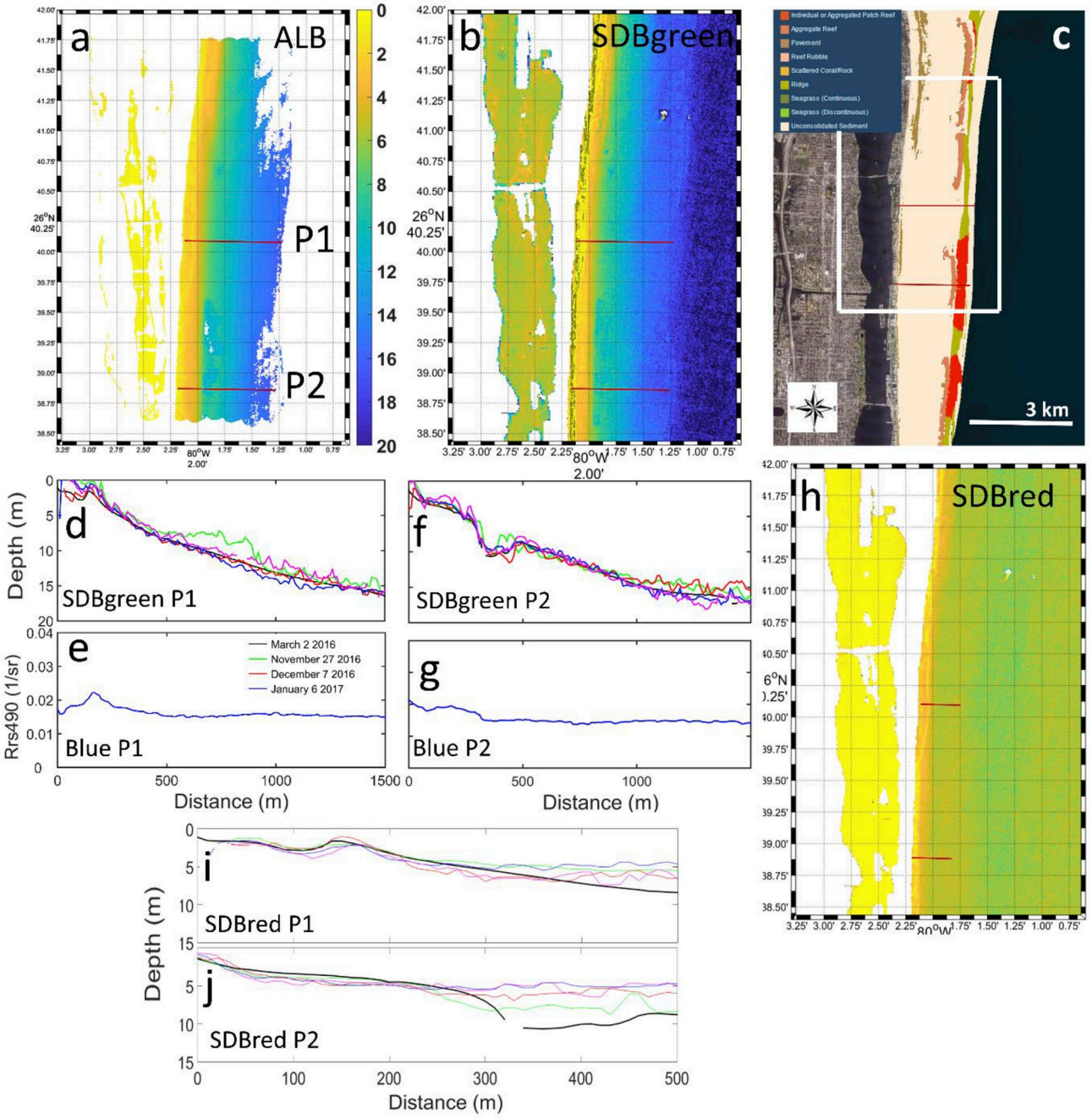

Fig. 4. (a) ALB in West Palm Beach indicating transects P1 and P2, (b) SDBgreen on 7 December 2016, (c) benthic habitat information corresponding to the Integrated Reef Map Project by the Florida Fish and Wildlife Conservation Commission, (d) and (f) detailed profiles of SDBgreen for P1 and P2, respectively, (e) and (g) profile of the blue band Rrs490 nm for P1 and P2, respectively; black line is ALB and the different colored lines correspond to the four MSI images, (h) SDBred on 7 December 2016, (i) and (j) profiles of SDBred for P1 and P2, respectively. Data in the maps is presented as colour coded depths ranging from 0 to 20 m.

Table 2
Tunable parameters scale and offset (m_1 and m_o, respectively), and coefficient of determination (r^2) defined for the vertical referencing of pSDBred (5 calibration points) and pSDBgreen (6 calibration points) for images acquired on 2 March, 27 November, 7 December 2016, and 6 January 2017 in West Palm Beach. The same in Key West on 8 February 2017 using 9 calibration points. The coefficients were retrieved using bands 445 nm and 490 nm for both SDB models. In addition, the calibration parameters are indicated for the scene on 7 December 2016 after surface reflectance correction for Test 1 and Test 2 (see specific results in Section 3.2).

Ratio model Original	$pSDBgreen_{445}$ (ALB = 0 18m)			$pSDBgreen_{490}$ (ALB = 0 18m)			$pSDBred_{445}$ (ALB = 0 6 m)			$pSDBred_{490}$ (ALB = 0 6 m)		
Parameter	m_0	m_1	r^2	m_0	m_1	r^2	m_0	m_1	r^2	m_0	m_1	r^2
2 March 2016	44.2	46.7	0.96	54.7	55.5	0.89	7.5	7.3	0.99	8.5	7.9	0.99
27 November 2016	42.8	43.7	0.87	55.8	56	0.74	5.8	5.1	0.87	5.5	5	0.85
7 December 2016	56.2	57.5	0.91	81.8	80.8	0.81	10.5	9.5	0.94	11.8	10.2	0.95
6 January 2017	42.6	44.7	0.96	58.5	58.1	0.93	6.5	5.5	0.89	7.6	5.5	0.79
8 February 2017	42.9	50.3	0.86	67.7	70.5	0.85	5.2	5.4	0.9	5.9	5.8	0.83
Surface reflectance correction 7 Dec.												
Test 1	44.4	45.8	0.89	59.9	59.1	0.84	5.9	5.4	0.88	7.2	6.5	0.8
Test 2	43.1	44.6	0.88	57.2	58.3	0.86	5.8	5.3	0.93	7.8	7	0.83

3.1.1. West Palm Beach

The first region corresponded to West Palm Beach (Figs. 1–4), which was characterized by a relatively constant slope in the ALB depths ranging from 0 to up to 18 m (Fig. 4a). Four images were selected under clear-sky conditions acquired on 2 March, 27 November, and, 7 December 2016, and 6 January 2017. Each scene was tuned separately using 445 nm or 490 nm bands in the algorithm (see calibration in Table 2). Comparison of SDB and ALB (Fig. 2) shows $SDBgreen_{445}$ (using band 445 nm) could consistently retrieve depths to at least 18 m (limit of the ALB survey) with Median Absolute Error (hereinafter MedAE) less than 1 m and specifically < 0.5 m on 27 November 2016. To look at different depth ranges the bias and MedAE were computed as statistics (Seegers et al., 2018) for 0–18 m and then partitioned to 0–5 m, 5–10 m and 10–18 m (Table 3 for band 445 nm, and Table 4 for band 490 nm). The error was linear over most of the range and depths up to 18 m were estimated with high consistency and accuracy for the different days. Minimum MedAE (< 0.3 m) was found for depths ranging between 10 and 18 m. Generally, higher errors (~1 m) were found for depths 0–5 m, as expected given that SDBgreen is more sensitive in deeper water. Similar performance was obtained with both blue bands, although slightly lower error for band 445 nm (Table 3) than for band 490 nm (Table 4). An additional exercise was accomplished comparing SDBgreen using band 490 nm against SDBgreen using band 445 nm for the scene acquired on 2 March 2016 (Fig. 3), indicating minimal differences with MedAE of 0.35 m and bias of −0.1 m.

Cross-shore profiles show the similarity between SDBgreen (Fig. 4b) and ALB (Fig. 4a) across the four scenes (Fig. 4d–f) and over different bottom types (Fig. 4c). Shallower than 2–3 m SDBgreen become unreliable, otherwise depth retrievals were possible up to the limit of lidar data at 18 m. On 2 March 2016 (profile P1, Fig. 4d) the depth was underestimated between 500 and 1000 m distance from shore due to higher turbidity levels. While SDBgreen did not retrieve reliably SDB in less than 2–3 m, SDBred (Fig. 4h) provided excellent estimation in those depths (Fig. 4i and j). SDBred measured to a maximum depth of about 5–6 m (see Tables 3 and 4 for statistics).

3.1.2. Key West

The second region of study was Key West, which has dynamic conditions that lead to moderately heterogeneous turbidity mainly in shallow areas (Jones and Boyer, 1998). The image on 8 February 2017, selected as the clearest scene in terms of clouds, sun glint, and turbidity, performed consistently over complex bathymetry and bottom types (Fig. 5). Because most of the ALB data ranged from 0 to 6 m (Fig. 5a), SDBred was used to derive the bathymetry (see Table 2 for calibration parameters). Errors were below 0.45 m using band 445 nm (bias = 0.13 m, MedAE = 0.42 m) or band 490 nm (bias = 0.27 m, MedAE = 0.39 m) in this area of complex bottom forms. Spatial features were well represented; the SDBred captured the tidal channels, as can be seen in the northern part (Fig. 5b). Similar to the West Palm Beach study, the depth penetration limit for SDBred was ~5 m for clearest waters (Fig. 4i and j). At depths greater than 5 m, SDBred began to fail, leading to underestimation, clearly observed at the top of the image. Most vertical features were well reproduced in the shallow basin, where bathymetry generated by MSI matched ALB in the cross-shore profiles (Fig. 5d–f). The algorithm captured the transition to deeper areas, evident in the steep slopes of both transects P1 (Fig. 5d) and P2 (Fig. 5e). These findings confirm that SDB retrieved from Sentinel-2 can provide valid bathymetric information including channels and straits relevant to navigation. Depths over several bottom types were present within this basin (Fig. 5c–g, seagrass, coral reef, unconsolidated sediment), which indicate the model resolved different substrate albedo, from vegetated to sandy or rocky bottoms. This consistent performance is apparent between 10 and 12 km in P1 and P2, where there is a large change from low to high values of reflectance at 490 nm (B02) associated with different bottom albedo (Stumpf et al., 2003) of seagrass, coral reef and sandy bottom (Fig. 5c), without comparable differences in the SDBred depths.

3.1.3. Dry Tortugas

The third tested region was the Dry Tortugas environment (Fig. 6a), which is frequently characterized by clear waters compared to Key West and West Palm Beach (Jones and Boyer, 1998). Severe cloud coverage

Table 3
Statistical analysis of the comparison between ALB and SDBgreen and SDBred derived from the MSI at 10 m spatial resolution in West Palm Beach. The units of bias and MedAE are meters. The band 445 nm was used in the ratio model.

Date	March, 2 2016			November 27, 2016			December 7, 2016			January 6, 2017		
SDBgreen	Bias (m)	MedAE (m)	n	Bias (m)	MedAE (m)	n	Bias (m)	MedAE (m)	n	Bias (m)	MedAE (m)	n
0–18 m	−0.82	0.78	76430	0.04	0.45	78741	0.06	0.51	78096	−0.24	0.58	76184
0–5 m	−0.93	0.85	16204	−0.15	0.46	16003	−0.58	0.70	14441	−0.32	0.78	14035
5–10 m	−0.69	0.72	20046	0.31	0.40	15667	0.29	0.29	19794	−0.21	0.54	23615
10–18 m	−0.83	0.78	40180	−0.03	0.48	47071	0.45	0.57	43861	−0.18	0.44	38534
SDBred												
0–6 m	−0.06	0.4	19801	−0.37	0.36	18430	−0.1	0.39	20342	0.09	0.41	19441

Table 4
Statistical analysis of the comparison between ALB and SDBgreen and SDBred derived from the MSI at 10 m spatial resolution in West Palm Beach. The units of bias and MedAE are meters. The band 490 nm was used in the ratio model.

Date	March, 2 2016			November 27, 2016			December 7, 2016			January 6, 2017		
SDBgreen	Bias (m)	MedAE (m)	n	Bias (m)	MedAE (m)	n	Bias (m)	MedAE (m)	n	Bias (m)	MedAE (m)	n
0–18 m	−0.72	0.72	78264	−0.2	0.6	78699	0.13	0.76	74653	−0.55	0.77	73725
0–5 m	−0.9	0.86	14504	−0.99	0.95	14653	−1.37	1.4	10619	−1.25	1.27	12507
5–10 m	−0.69	0.7	20577	0.2	0.43	20776	−0.25	0.41	20776	−0.33	0.61	19744
10–18 m	−0.62	0.64	43183	0.18	0.54	43270	0.67	0.88	43258	−0.35	0.74	41474
SDBred												
0–6 m	0.21	0.51	19820	−0.23	0.3	18430	−0.25	0.38	20340	−0.13	0.5	19446

in this region limited the acquisition of a clear scene. Since the majority of the ALB ranged only from 0 to 6 m (Fig. 6c), SDBred was used in this case as in Key West. The MSI bathymetric map for an image acquired on 8 February 2017 (Fig. 6d) provided good accuracy up to 6 m with MedAE of 0.22 m and bias of −0.15 m (N = 419306). The calibration parameters were 4.1 and 3.7 for offset and slope, respectively, using five control points. The scatter against ALB (Fig. 6g) reflected accuracy and minimum errors, where slight underestimation occurred in regions of ALB > 5 m. The profiles in Fig. 6e and f further confirmed the good performance of the ratio model over different bottom substrates, where there is a large change from low to high values of reflectance at 490 nm (B02) associated with different bottom albedo of seagrass, coral reef, and sandy bottom (Fig. 6f), without comparable differences in the SDBred depth (Fig. 6e).

3.2. Satellite-Derived Bathymetry for recursive retrieval

An analysis of SDB mapping focused on West Palm Beach (large range of ALB) was conducted to determine the repeatability and consistency of the approach. Each image in this site was tuned independently in the previous section 3.1.1. For recursive SDB retrieval, consistency was examined by using only one generic tuning implemented for all the images. The calibration between the pSDB values and the chart sounding is a critical step in the SDB models,

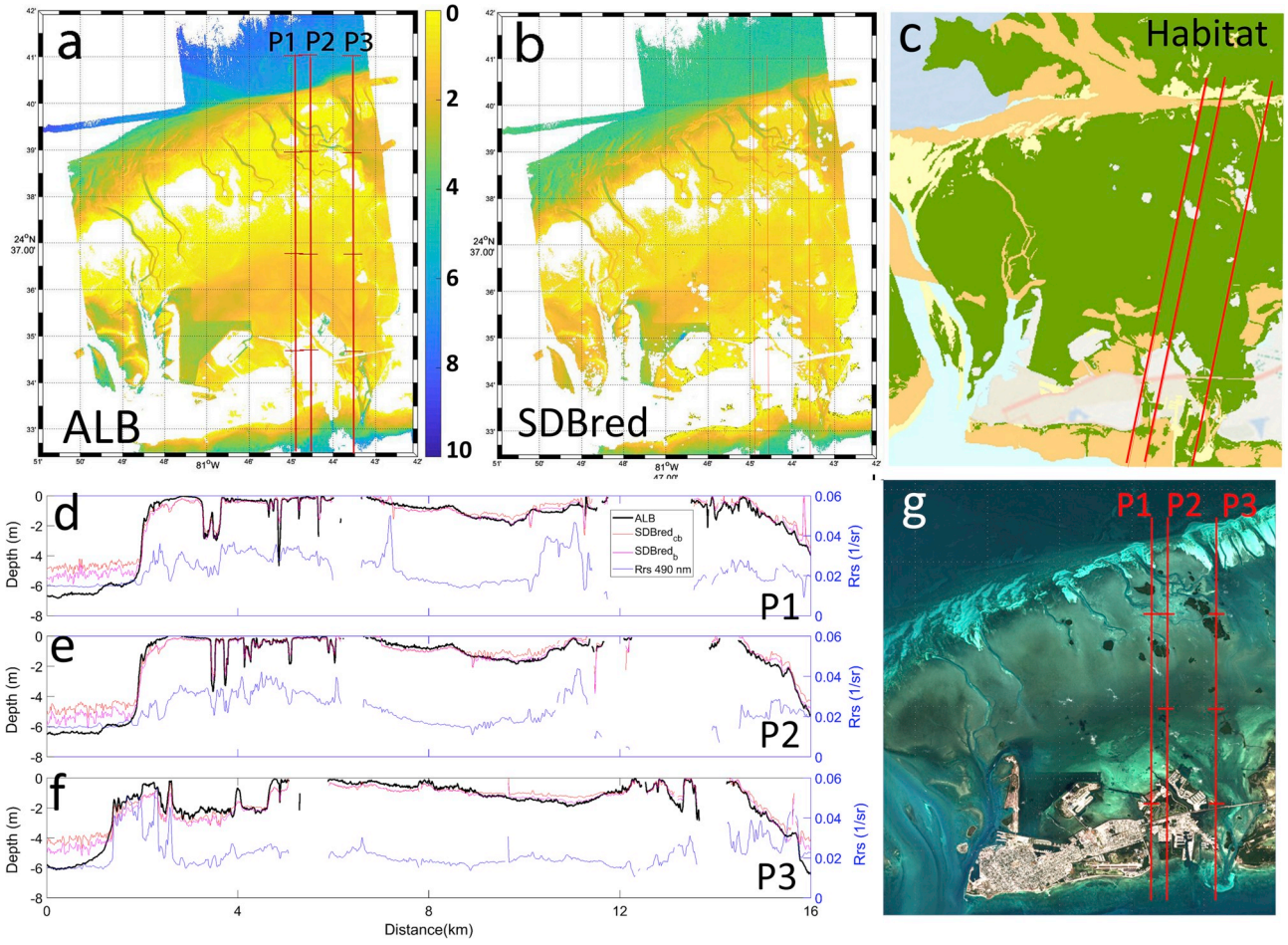

Fig. 5. (a) ALB in Key West indicating transects P1, P2 and P3, (b) SDBred derived from MSI for an image acquired on 8 February 2017 (using band 445 nm). White pixels represent depths derived as situated above the sea surface or masked after ACOLITE processor, (c) benthic habitats of the Lower Keys and Key West by NOAA (yellow, unconsolidated sediment; green, seagrass; orange, coral reef and hard bottom; blue, not classified), (d), (e), and (f) three profiles for ALB (black line), SDBred (red line is using band 445 nm, magenta line is using band 490 nm), and reflectance of the 490 nm band Rrs490 (blue line) along P1, P2, and P3, respectively, (g) Red-Green-Blue (RGB) composite of MSI on 8 February 2017 showing the three cross-shore profiles (P1-P3).

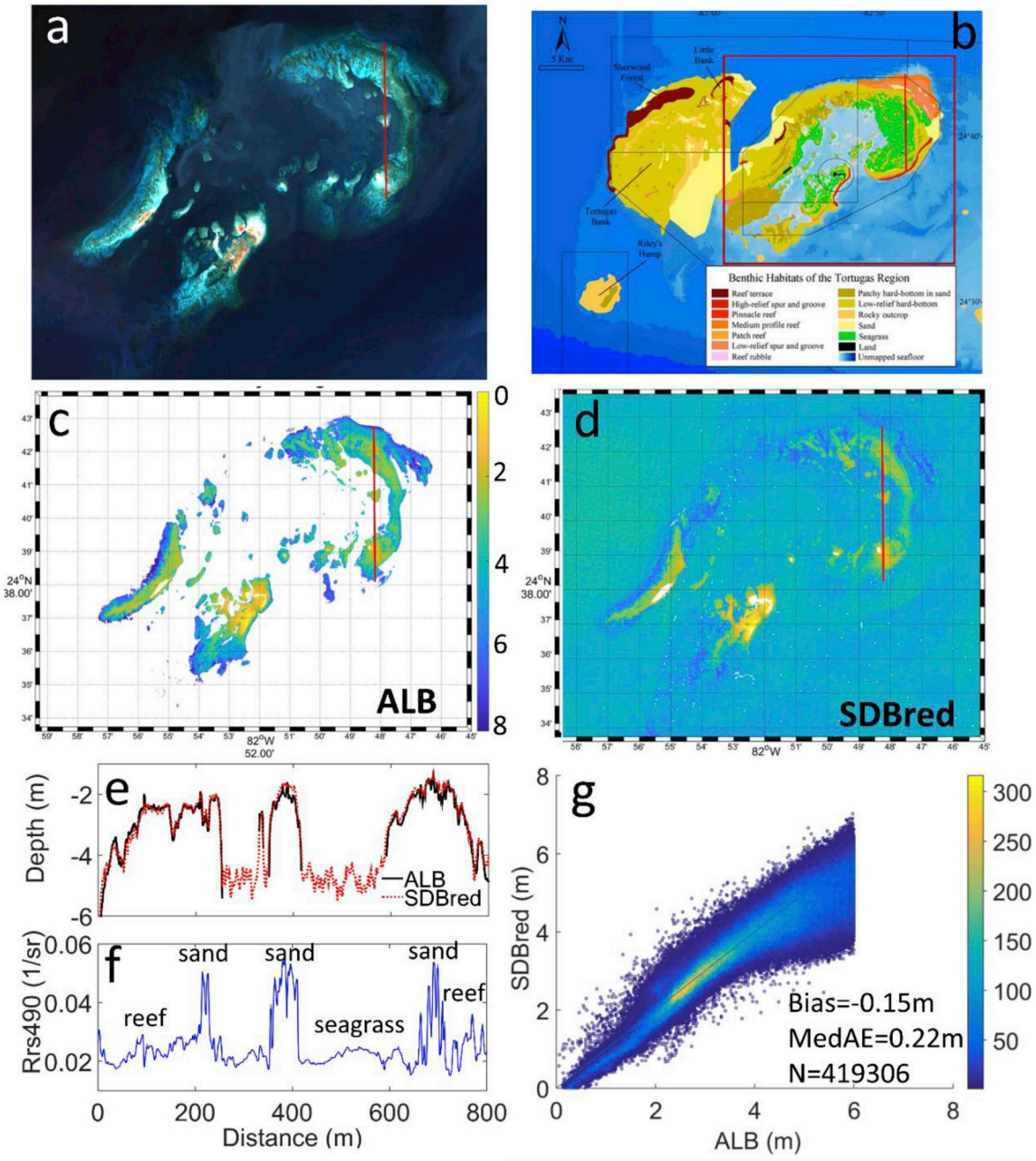

Fig. 6. a) RGB composite derived from a MSI image acquired on 8 February 2017 in Dry Tortugas, b) benthic habitats from Franklin et al. (2003); red rectangle indicates the study region for SDB, c) ALB; d) SDBred on 8 February 2017 (using band 490 nm); white pixels represent depths derived as situated above the sea surface or masked after ACOLITE processor, e) depth transect of ALB (back line) and SDBred (red line), f) profile of the blue bands at 490 nm, g) scatter plot of ALB against SDBred for depths 0–6m.

Table 5
Statistical analysis of the comparison between ALB and SDBgreen (using band 445 nm) derived from the MSI at 10 m spatial resolution in West Palm Beach for March 2, November 27, and December 7, 2016. The calibration coefficients used for the generic vertical tuning (6 January 2017 as the reference image) are m_0 = 42.6 and m_1 = 44.7 (Table 2).

Date	March 2, 2016			November 27, 2016			December 7, 2016		
SDBgreen	Bias (m)	MedAE (m)	n	Bias (m)	MedAE (m)	n	Bias (m)	MedAE (m)	n
0–18 m	−1.1	1.04	75969	1.42	1.32	80663	−0.71	0.8	81016
0–5 m	−1.12	1.02	14748	1.1	1.01	11804	−0.16	0.45	16918
5–10 m	−1.11	1.11	25527	1.49	1.41	14353	−0.64	0.7	27869
10–18 m	−1.03	1.02	35694	1.65	1.52	54506	−1.31	1.24	36229

incorporating differences in water level (micro-tidal regime) and water transparency conditions. For this examination, the 6 January 2017 scene was chosen as the reference, and its tuning coefficients were applied to the other images (Table 5). While the error increased slightly, the median error was still ~1 m for depths 0–18 m compared to the targeted tuning with median errors ~0.5 m (Table 3).

Except December 2016, all scenes had quite similar coefficients (Table 2). The difference for the December 2016 scene can be associated with a residual error after ACOLITE, probably due to residual uncorrected aerosol. Residual surface reflectance is unlikely; November, December and January have the same sun angles and no residual surface reflectance was evident. A different aerosol type than applied may have caused the December 2016 artifact. For other times of year with higher sun angles, surface reflectance should be considered, as this version of ACOLITE did not include a correction for surface reflectance or wave facets. To correct for residual aerosol signal before SDB retrieval, two straightforward exercises were developed using the image on 6 January 2017 as a reference and the image in December 2016 as the testing scene. The first one (Test1) corresponded to a pixel by pixel subtraction of Rrs704 for December 2016 from all channels but adding back in the mode of January 2017 (Stumpf and Pennock, 1989; Hochberg et al., 2003), and the second (Test2) corresponded to a pixel by pixel subtraction of 0.5*Rrs704 for December 2016 from all channels. The two approaches provided similar SDBgreen coefficients to the reference scene (Table 2). The median errors ~0.5 (Table 6) were comparable between depth ranges and equivalent to the ones stated in Tables 3 and 5. Similar results were obtained using the reflectance at 740 nm (Rrs740) instead of Rrs704 (not included here). Therefore, not correcting for residual aerosol signal in the reflectance did allow determination of depths. However, correcting for it increased consistency in the calibration, permitting the use of a generic calibration across all the scenes with similar sun angle.

3.3. Comparison of Sentinel-2A and 2B satellites

Previous analysis of SDB validation (Section 3.1 and 3.2) with ALB were focused on Sentinel-2A satellite before Hurricane Irma reached the Keys in September 2017, since intense resuspension and currents may have modified shallow seabed morphology, confounding comparison with the lidar survey. However, given that the first images of Sentinel-2B in SF were obtained after Irma, additional imagery was selected after September 2017 for examination of Sentinel-2A and 2B consistency and similarity. Two clear scenes for each satellite were selected in West Palm Beach and Dry Tortugas for SDBgreen and SDBred evaluation, respectively, during the same period in 2017 (within ~15 days of difference). The scatter plots indicate similar performance between both MSI sensors with MedAE of 0.64 in West Palm (Fig. 7a) and 0.26 m in Dry Tortugas (Fig. 7b) lying on the 1:1 line. Slightly higher errors were encountered for these scenes in both study locations (see calibration parameters and validation performance in Table 7), which may be related to bottom erosion/sedimentation after Irma not accounted in ALB. These results are encouraging for future implementation of multi-sensor approaches with both MSI instruments, thus confirming for first time, to the best of our knowledge, the potential of applying Sentinel-2A and 2B as interchangeable satellites for bathymetric mapping.

Table 6
Statistical analysis of the comparison between ALB and SDBgreen and SDBred (using band 445 nm) in West Palm Beach in 7 December 2016. Test1 and Test2 corresponded to the surface reflectance correction described in the text. The calibration coefficients are indicated in Table 2.

SDBgreen	Test1		Test2	
	Bias (m)	MedAE(m)	Bias (m)	MedAE (m)
0–18 m	−0.17	0.56	−0.18	0.52
0–5 m	−0.76	0.81	−0.65	0.81
5–10 m	−0.11	0.33	−0.19	0.33
10–18 m	0.34	0.55	0.28	0.47
SDBred				
0–6 m	0.65	0.81	−0.095	0.35

4. Discussion

This study shows the potential of Sentinel-2A/B imagery to successfully map bathymetry at 10 m spatial resolution over shallow optical regions in South Florida with conditions of low turbidity (Jones and Boyer, 1998). Accurate SDB products could be retrieved using the ratio algorithm with both models, SDBred (ratio of the blue to red bands) for depths up to 6 m, and SDBgreen (ratio of the blue to green bands) for depths to at least 18 m (limit of validation data). SDBred was sensitive in waters < 5–6 m in the three study sites while SDBgreen performed poorly at depths < 3 m in West Palm Beach. Replacing the green band with red should aid in retrieving depths in shallow highly reflective waters. This approach was implemented by NOAA in the Atlas of the shallow NW Hawaiian Islands (National Oceanic and Atmospheric Administration-NOAA, 2003), where the blue to red ratio substituted for the blue to green ratio algorithm for waters < 5 m. The overlapping depth range (3–5 m) between both models can allow for inter-comparison of bathymetric retrievals. The results also suggest that a merged switching method would be appropriate in these environments with SDBred applied in shallow waters (< 5 m) and SDBgreen in deep waters (> 5 m).

Bathymetry mapping with Sentinel-2A/B at 10 m has an advantage in comparison with Landsat-8 at 30 m (Pe'eri et al., 2014; Pacheco et al., 2015; Kabiri, 2017a), particularly in retrieving more features (Hedley et al., 2018). The utility of Sentinel-2A/B is clearly observed in Key West (Fig. 5) and Dry Tortugas (Fig. 6), where the scale of nearshore complex geomorphological features such as the narrow channels and steep slopes were mapped with the MSI. In addition, depths were retrieved with errors < 1m in these areas with variable bottom types (e.g., hard-bottom, soft-sediment and sandy bottom types, mainly carbonates, seagrass, and coral reef) (Fourqurean et al., 1992; Franklin et al., 2003; Finkl and Warner, 2005).

The coastal blue band at 445 nm (B01) and the standard blue at 490 nm (B02) yielded similar performances. Slightly lower error was encountered for band 445 nm; however, the 445 nm band has substantially lower raw resolution (60 m), so there is little to be gained by using it for routine mapping in these water depths. In addition, we have also confirmed that ACOLITE produced a robust and consistent atmospheric correction for both Sentinel-2A and 2B satellites over different locations and scenes. Noise by MSI appeared enhanced for deeper waters. Some of this noise might be associated with the remaining noise or possibly surface reflectance (specular reflection) not removed after the median filtering applied to ACOLITE outputs. Minghelli-Roman et al. (2009) suggested constant, random and quantization noises need to be reduced as much as possible in order to obtain sufficient depth accuracy from deeper waters. Scene surface reflection (NIR residual reflectance) was implicitly removed from the SDB with the atmospheric correction. However, directly removing the surface reflectance by a pixel-based correction (similar to Hochberg et al., 2003 and Stumpf and Pennock, 1989) indicated that retuning the coefficients for this problem was not necessary, with the same overall errors at different depth ranges (Tables 5-6).

The ratio transform required tuning of only two parameters. We utilized available sounding data from several updated and reliable NOAA charts to calculate the empirical coefficients, using only 5 to 10 points for each model (the original algorithm used 5 depths from existing paper charts – one estimated as zero). For practical application in remote areas, this is a key benefit, especially where one tuning could be applied across multiple scenes without increasing error above 1 m. For

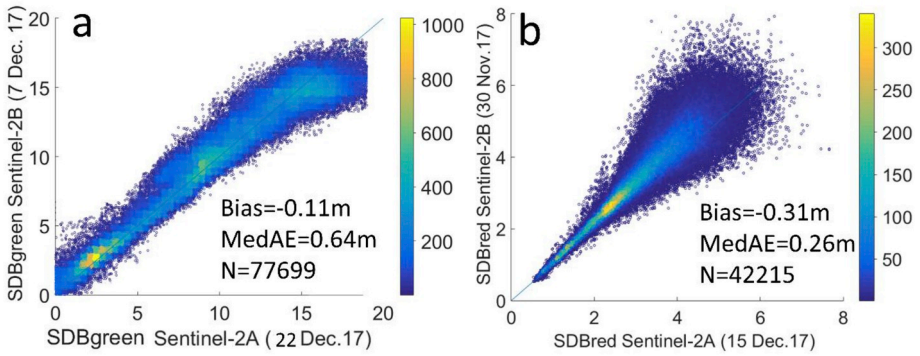

Fig. 7. Scatterplot of comparison between Sentinel-2A and 2B for (a) SDBgreen in West Palm Beach, and (b) SDBred in the Dry Tortugas, for scenes acquired within a few weeks in 2017. The band 490 nm was used in the ratio model.

areas without any soundings, a satellite model may provide reference data. A recent publication by the International Hydrographic Organization (International Hydrographic Review, 2014) addressed the need to improve the collection, quality and availability of hydrographic data worldwide, while monitoring and rectifying possible deficiencies and shortcomings that are presented on the charts. In the opinion of the IHO, shallow water bathymetry derived from multi-spectral imagery should be considered as a potential technology for obtaining bathymetry for charting purposes in areas where existing surveys are poor or non-existent. This work indicates that an existing calibration can be used for recursive mapping in one region. Evaluating the application of existing calibrations to new sites will be an important area of research in order to apply the SDB to regions where soundings are rare.

The Sentinel-2 mission specification of 5-day revisit at the Equator offers a new capability in routine Earth Observation. Both twin satellites yield a major number of images, which will be helpful for enhancing SDB estimations in regions with severe cloud coverage, ice cover or sun glint issues. Casal et al. (2019) used Sentinel-2A data in two study areas of the Irish coast with RMSE ~1.4 m for depths up to 10 m, suggesting that atmospheric correction and water column conditions proved to be key factors in the bathymetric derivation. A recent study using the geospatial platform of the Google Earth Engine (GEE) estimated SDB with Sentinel-2A in three sites in the Eastern Mediterranean with RMSE ~1.5 m (Traganos et al., 2018). In addition, a bathymetric retrieval algorithm developed to a subset of Sentinel-1 over the North Sea demonstrated the suitability of the technique in working with Synthetic Aperture Radar (SAR) data, revealing the same pattern of bathymetric features at an initial water depth of around 15–25 m (Stewart et al., 2016). Our demonstration of interchangeable use of the two satellites for SDB mapping is critical to successful routine monitoring. The Sentinel-2 constellation will benefit temporal studies requiring yearly or more frequent update of bathymetric data in rapidly varying aquatic systems such as rivers, tidal channels, underwater sand dunes, dredged ports, or after the passage of hurricanes/tropical storms. Pe'eri et al. (2014) already demonstrated multi-temporal SDB approaches produced better monitoring data quality as well as allowed error analysis. This methodology should be applicable to very high resolution satellites (Stumpf et al., 2003; Eugenio et al., 2015; Hamylton et al., 2015; Halls and Costin, 2016), which may allow integration of these sensors with the more routine Sentinel-2 products.

5. Conclusions

The results of this study demonstrate the capability of Sentinel-2 twin mission in generating essential bathymetric information at 10 m spatial resolution in three different sites. The atmospheric correction by means of ACOLITE software and the use of the ratio model enable excellent bottom mapping to at least 18 m with error ~0.5 m. Repeatability and accuracy of SDB retrievals has been also verified through these approaches, where few calibration points (5–10) are needed from chart soundings. MSI can capture small-scale features, such as tidal channels, straits relevant to navigation or steep slopes, due to its fine spatial resolution. These findings are encouraging for future implementation of multi-sensor analysis, addressing the potential of using Sentinel-2A and 2B as interchangeable satellites for SDB mapping.

This approach represents a new perspective for remotely sensed seabed topography extraction with high level of accuracy and with the advantages of a fast, flexible, and economically advantageous solution over broad areas. Consequently, the Sentinel-2 set of derived information will generate reciprocal benefit for improved competiveness of coastal and inland bathymetric products and their future evolution, contributing to the advancements for environmental management, monitoring, modelling, and for scientific purposes, especially in remote areas and developing countries.

Acknowledgements

We thank the European Space Agency and the Copernicus programme for distributing Sentinel-2A/B imagery. Thanks to the National Geodetic Survey and the National Oceanic and Atmospheric Administration for providing the valuable high-resolution lidar data and nautical charts used for this study. Thanks to Quinten Vanhellemont for his assistance in using ACOLITE processor. The authors acknowledge the two anonymous reviewers, whose comments helped to improve this manuscript. Isabel Caballero is funded by the National Oceanic and Atmospheric Administration and the National

Table 7
Calibration coefficients for Sentinel-2A and 2B, and statistical comparison against ALB of SDBgreen in West Palm Beach and SDBred in the Dry Tortugas. The band 490 nm was used in the ratio model. Calibration parameters (m_0 and m_1) and coefficient of correlation (r^2) for the calibration in each site and SDB model are presented.

Study Site	Satellite	Date	MedAE (m)	Bias (m)	n	m_0	m_1	r^2
West Palm	2B	Dec.17, 7	0.91	−0.61	77256	37.9	43.5	0.89
West Palm	2A	Dec.17, 22	1.01	−0.3	78023	44.6	47	0.81
Dry Tortugas	2B	Nov.17, 30	0.27	0.027	413212	2.9	3.1	0.94
Dry Tortugas	2A	Dec.17, 15	0.30	−0.24	406589	2.2	2.6	0.85

Academy of Science, Engineering and Medicine under the NRC post-doctoral Research Associateship Program (RAP) 2017–2019. Support was also provided by the Korean Hydrographic and Oceanographic Administration. The research was also supported by the Sen2Coast project (RTI2018-098784-J-I00) under the Spanish Ministry of Science R+D Projects "Challenges of Society" for young investigators (2019-2022).

Appendix A. Supplementary data

Supplementary data to this article can be found online at https://doi.org/10.1016/j.ecss.2019.106277.

References

Barnes, B.B., Hu, C., 2013. A hybrid cloud detection algorithm to improve MODIS sea surface temperature data quality and coverage over the Eastern Gulf of Mexico. IEEE Trans. Geosci. Remote Sens. 51 (6), 3273–3285.
Benedet, L., Finkl, C.W., Klein, A., 2004. Classification of Florida Atlantic beaches: sediment variation, morphodynamics, and coastal hazards. J. Coast. Res. 120–129.
Benny, A.H., Dawson, G.J., 1983. Satellite imagery as an aid to bathymetric charting in the Red Sea. Cartogr. J. 20 (1), 5–16.
Bramante, J.F., Raju, D.K., Sin, T.M., 2013. Multispectral derivation of bathymetry in Singapore's shallow, turbid waters. Int. J. Remote Sens. 34 (6), 2070–2088.
Brando, V.E., Anstee, J.M., Wettle, M., Dekker, A.G., Phinn, S.R., Roelfsema, C., 2009. A physics based retrieval and quality assessment of bathymetry from suboptimal hyperspectral data. Remote Sens. Environ. 113 (4), 755–770.
Caballero, I., Steinmetz, F., Navarro, G., 2018. Evaluation of the first year of operational Sentinel-2A data for retrieval of suspended solids in medium-to high-turbidity waters. Rem. Sens. 10 (7), 982.
Casal, G., Monteys, X., Hedley, J., Harris, P., Cahalane, C., McCarthy, T., 2019. Assessment of empirical algorithms for bathymetry extraction using Sentinel-2 data. Int. J. Remote Sens. 40 (8), 2855–2879.
Chybicki, A., 2017. Mapping South baltic near-shore bathymetry using sentinel-2 observations. Pol. Marit. Res. 24 (3), 15–25.
Clark, R.K., Fay, T.H., Walker, C.L., 1988. Bathymetry using thematic mapper imagery. In: Ocean Optics IX, 925, 229-232, International Society for Optics and Photonics.
Culver, M., Schubel, J., Davidson, M., Haines, J., 2010. Building a sustainable community of coastal leaders to deal with sea level rise and inundation. In: Proceedings from the Sea Level Rise and Inundation Community Workshop, Lansdowne, MD, Dec 3-5, 2009. Sponsored by the National Oceanic and Atmospheric Administration and U.S. Geological Survey.
Dekker, A.G., Phinn, S.R., Anstee, J., Bissett, P., Brando, V.E., Casey, B., et al., 2011. Intercomparison of shallow water bathymetry, hydro-optics, and benthos mapping techniques in Australian and Caribbean coastal environments. Limnol Oceanogr. Methods 9 (9), 396–425.
Drusch, M., Gascon, F., Berger, M., 2010. GMES Sentinel-2 Mission Requirements Document. ESA EOP-SM1163MR-Dr2 42.
Duane, D.B., Meisburger, E.P., 1969. Geomorphology and Sediments of the Nearshore Continental Shelf, Miami to Palm Beach, Florida (No. TM-29). Army Coastal Engineering Research Center, Washington DC.
Eugenio, F., Marcello, J., Martin, J., 2015. High-resolution maps of bathymetry and benthic habitats in shallow-water environments using multispectral remote sensing imagery. IEEE Trans. Geosci. Remote Sens. 53 (7), 3539–3549.
European Space Agency, 2015. Sentinel-2 User Handbook. ESA Standard Document; ESA, Paris, France.
Finkl, C.W., Warner, M.T., 2005. Morphologic features and morphodynamic zones along the inner continental shelf of southeastern Florida: an example of form and process controlled by lithology. J. Coast. Res. 79–96.
Fourqurean, J.W., Zieman, J.C., Powell, G.V., 1992. Phosphorus limitation of primary production in Florida Bay: evidence from C: N: P ratios of the dominant seagrass Thalassia testudinum. Limnol. Oceanogr. 37 (1), 162–171.
Franklin, E.C., Ault, J.S., Smith, S.G., Luo, J., Meester, G.A., Diaz, G.A., et al., 2003. Benthic habitat mapping in the Tortugas region, Florida. Mar. Geod. 26 (1–2), 19–34.
Gao, J., 2009. Bathymetric mapping by means of remote sensing: methods, accuracy and limitations. Prog. Phys. Geogr. 33 (1), 103–116.
Guenther, G.C., 2011. Airborne Lidar Bathymetry. Digital Elevation Model Technologies and Applications: the DEM Users Manual. In: Maune, David F. (Ed.), first ed. Bethesda, MD: American Society for Photogrammetry and Remote Sensing, pp. 237–306.
Halls, J., Costin, K., 2016. Submerged and emergent land cover and bathymetric mapping of estuarine habitats using worldview-2 and LiDAR imagery. Rem. Sens. 8 (9), 718.
Hamylton, S.M., Hedley, J.D., Beaman, R.J., 2015. Derivation of high-resolution bathymetry from multispectral satellite imagery: a comparison of empirical and optimisation methods through geographical error analysis. Rem. Sens. 7 (12), 16257–16273.
Hedley, J.D., Roelfsema, C., Brando, V., Giardino, C., Kutser, T., Phinn, S., et al., 2018. Coral reef applications of Sentinel-2: coverage, characteristics, bathymetry and benthic mapping with comparison to Landsat 8. Remote Sens. Environ. 216, 598–614.
Hochberg, E.J., Andréfouët, S., Tyler, M.R., 2003. Sea surface correction of high spatial resolution Ikonos images to improve bottom mapping in near-shore environments. IEEE Trans. Geosci. Remote Sens. 41 (7), 1724–1729.
International Hydrographic Review, May, 2014. Report by Ian Halls, Editor.
IOCCG, 2000. Remote Sensing of Ocean Colour in Coastal, and Other Optically-Complex, Waters. IOCCG S. Sathyendranath Dartmouth, Canada.
Islam, S., Hasan, Z., Islam, A., 2016. The challenges of river bathymetry survey using Space borne remote sensing in Bangladesh. Atmos. Ocean Sci. 1 (1), 7–13.
Jawak, S.D., Vadlamani, S.S., Luis, A.J., 2015. A synoptic review on deriving bathymetry information using remote sensing technologies: models, methods and comparisons. Adv. Rem. Sens. 4 (02), 147.
Jones, R., Boyer, J.N., 1998. Florida Keys National Marine Sanctuary Water Quality Monitoring Project: 1998 Annual Report.
Kabiri, K., 2017a. Accuracy assessment of near-shore bathymetry information retrieved from Landsat-8 imagery. Earth Sci. India 10 (2), 235–245.
Kabiri, K., 2017b. Discovering optimum method to extract depth information for near-shore coastal waters from Sentinel-2A imagery-case study: nayband Bay, Ian. International Archives of the Photogrammetry. Remote Sens. Spat. Inf. Sci. 42.
Kao, H.M., Ren, H., Lee, C.S., Chang, C.P., Yen, J.Y., Lin, T.H., 2009. Determination of shallow water depth using optical satellite images. Int. J. Remote Sens. 30 (23), 6241–6260.
Kanno, A., Tanaka, Y., Shinohara, R., Kurosawa, A., Sekine, M., 2014. Which spectral bands of Worldview-2 are useful in remote sensing of water depth? A case study in coral reefs. Mar. Geod. 37 (3), 283–292.
Khondoker, M.S.I., Siddiquee, M.Z.H., Islam, M., 2016. The challenges of river bathymetry survey using Space borne remote sensing in Bangladesh. Atmos. Ocean Sci. 1 (1), 7–13.
Lafon, V., Froidefond, J.M., Lahet, F., Castaing, P., 2002. SPOT shallow water bathymetry of a moderately turbid tidal inlet based on field measurements. Remote Sens. Environ. 81 (1), 136–148.
LaPointe, B.E., Clark, M., 1992. Nutrient inputs from the watershed and coastal eutrophication in the Florida Keys. Estuar. Coasts 15, 465–476.
Lee, Z., Carder, K.L., Mobley, C.D., Steward, R.G., Patch, J.S., 1999. Hyperspectral remote sensing for shallow waters: 2. Deriving bottom depths and water properties by optimization. Appl. Optic. 38 (18), 3831–3843.
Lee, Z., Casey, B., Arnone, R.A., Weidemann, A.D., Parsons, R., Montes, M.J., et al., 2007. Water and bottom properties of a coastal environment derived from Hyperion data measured from the EO-1 spacecraft platform. J. Appl. Remote Sens. 1 (1), 011502.
Lyzenga, D.R., 1981. Remote sensing of bottom reflectance and water attenuation parameters in shallow water using aircraft and Landsat data. Int. J. Remote Sens. 2 (1), 71–82.
Lyzenga, D.R., Malinas, N.P., Tanis, F.J., 2006. Multispectral bathymetry using a simple physically based algorithm. IEEE Trans. Geosci. Remote Sens. 44 (8), 2251–2259.
Maritorena, S., Morel, A., Gentili, B., 1994. Diffuse reflectance of oceanic shallow waters: influence of water depth and bottom albedo. Limnol. Oceanogr. 39 (7), 1689–1703.
Martins, V.S., Barbosa, C.C.F., de Carvalho, L.A.S., Jorge, D.S.F., Lobo, F.D.L., Novo, E.M.L.D.M., 2017. Assessment of atmospheric correction methods for sentinel-2 MSI images applied to amazon floodplain lakes. Rem. Sens. 9 (4), 322.
Minghelli-Roman, A., Goreac, A., Mathieu, S., Spigai, M., Gouton, P., 2009. Comparison of bathymetric estimation using different satellite images in coastal sea waters. Int. J. Remote Sens. 30 (21), 5737–5750.
National Oceanic and Atmospheric Administration-NOAA, 2003. Atlas of the Shallow-Water Benthic Habitats of the Northwestern Hawaiian Islands. pp. 160.
Pacheco, A., Horta, J., Loureiro, C., Ferreira, Ó., 2015. Retrieval of nearshore bathymetry from Landsat 8 images: a tool for coastal monitoring in shallow waters. Remote Sens. Environ. 159, 102–116.
Pahlevan, N., Sarkar, S., Franz, B.A., Balasubramanian, S.V., He, J., 2017b. Sentinel-2 MultiSpectral Instrument (MSI) data processing for aquatic science applications: demonstrations and validations. Remote Sens. Environ. 201, 47–56.
Pahlevan, N., Schott, J.R., Franz, B.A., Zibordi, G., Markham, B., Bailey, S., et al., 2017a. Landsat 8 remote sensing reflectance (Rrs) products: evaluations, intercomparisons, and enhancements. Remote Sens. Environ. 190, 289–301.
Pe'eri, S., Azuike, C., Alexander, L., Parrish, C., Armstrong, A., 2012. Beyond the chart: the use of satellite remote sensing for assessing chart adequacy and completeness information. In: Proceedings of the 2012 Canadian Hydrographic Conference: the Arctic, Old Challenges, New Approaches, Niagara Falls, Canada, pp. 15–17.
Pe'eri, S., Parrish, C., Azuike, C., Alexander, L., Armstrong, A., 2014. Satellite remote sensing as a reconnaissance tool for assessing nautical chart adequacy and completeness. Mar. Geod. 37 (3), 293–314.
Philpot, W.D., 1989. Bathymetric mapping with passive multispectral imagery. Appl. Optic. 28 (8), 1569–1578.
Robinson, J.A., Feldman, G.C., Kuring, N., Franz, B., Green, E., Noordeloos, M., Stumpf, R.P., 2000. Data fusion in coral reef mapping: working at multiple scales with SeaWiFS and astronaut photography. In: Proceedings of the 6th International Conference on Remote Sensing for Marine and Coastal Environments. 2. pp. 473–483.
Ruddick, K., Vanhellemont, Q., Dogliotti, A., Nechad, B., Pringle, N., Van der Zande, D., 2016. New opportunities and challenges for high resolution remote sensing of water colour. In: Ocean Optics 2016, Canada.
Seegers, B., Stumpf, R., Schaeffer, B., Loftin, K., Werdell, J., 2018. Performance metrics for the assessment of satellite data products: an ocean color case study. Optic Express 26 (6), 7404–7422.
Staff, D., 2013. The Benefits of the 8 Spectral Bands of WorldView-2: Applications Whitepaper. DigitalGlobe, London, pp. 12 Technical Report WP-8SPEC Rev 01/13.
Stewart, C., Renga, A., Gaffney, V., Schiavon, G., 2016. Sentinel-1 bathymetry for North Sea palaeolandscape analysis. Int. J. Remote Sens. 37 (3), 471–491.
Stumpf, R.P., Pennock, J.R., 1989. Calibration of a general optical equation for remote

sensing of suspended sediments in a moderately turbid estuary. J. Geophys. Res.: Oceans 94 (C10), 14363–14371.
Stumpf, R.P., Holderied, K., Sinclair, M., 2003. Determination of water depth with high-resolution satellite imagery over variable bottom types. Limnol. Oceanogr. 48 (1part2), 547–556.
Toming, K., Kutser, T., Laas, A., Sepp, M., Paavel, B., Nõges, T., 2016. First experiences in mapping lake water quality parameters with Sentinel-2 MSI imagery. Rem. Sens. 8 (8), 640.
Traganos, D., Reinartz, P., 2017. Mapping mediterranean seagrasses with sentinel-2 imagery. Mar. Pollut. Bull. 134, 197–209.
Traganos, D., Poursanidis, D., Aggarwal, B., Chrysoulakis, N., Reinartz, P., 2018. Estimating satellite-derived bathymetry (SDB) with the Google Earth engine and sentinel-2. Rem. Sens. 10 (6), 859.
Vanhellemont, Q., Ruddick, K., 2016. Acolite for sentinel-2: aquatic applications of MSI imagery. In: Proceedings of the ESA Living Planet Symposium, 9-13, Prague, Czech Republic.